CHEMISTRY

Low temperature rates for key steps of interstellar gas-phase water formation

Sunil S. Kumar[1]*†, Florian Grussie[1], Yury V. Suleimanov[2,3]†, Hua Guo[4], Holger Kreckel[1]†

The gas-phase formation of water molecules in the diffuse interstellar medium (ISM) proceeds mainly via a series of reactions involving the molecular ions OH^+, H_2O^+, and H_3O^+ and molecular hydrogen. These reactions form the backbone for the chemistry leading to the formation of several complex molecular species in space. A comprehensive understanding of the mechanisms involved in these reactions in the ISM necessitates an accurate knowledge of the rate coefficients at the relevant temperatures (10 to 100 K). We present measurements of the rate coefficients for two key reactions below 100 K, which, in both cases, are significantly higher than the values used in astronomical models thus far. The experimental rate coefficients show excellent agreement with dedicated theoretical calculations using a novel ring-polymer molecular dynamics approach that offers a first-principles treatment of low-temperature barrierless gas-phase reactions, which are prevalent in interstellar chemical networks.

INTRODUCTION

Water—one of the most important molecules for life as we know it—has been observed in the interstellar medium (ISM) in gaseous and solid forms (*1*–*3*). In the diffuse ISM, ion-neutral reactions at low temperature (10 to 100 K) are the driving force for the formation of more complex molecules in space. Under these conditions, water is formed mainly via a chain of exothermic gas-phase processes with no intrinsic barriers (*4*)

$$OH^+ + H_2 \rightarrow H_2O^+ + H \quad (1)$$

$$H_2O^+ + H_2 \rightarrow H_3O^+ + H \quad (2)$$

$$H_3O^+ + e^- \rightarrow H_2O + H \quad (3)$$

where the hydroxyl ion OH^+ is formed either by the reaction of O^+ with molecular hydrogen or by the reaction of atomic oxygen with H_3^+. The O^+ ions are created by charge-transfer reactions between atomic oxygen and atomic hydrogen ions that are produced by cosmic ray ionization, whereas the H_3^+ formation is initiated by cosmic ray ionization of H_2. Consequently, the formation of OH^+, H_2O^+, and H_3O^+ are all essentially cosmic ray–driven, and one can use their abundance to constrain the cosmic ray ionization rate in the diffuse ISM and the fraction of atomic to molecular hydrogen (*4*, *5*).

All three molecular ions, OH^+, H_2O^+, and H_3O^+, have been observed in the ISM, often in surprisingly high abundance. OH^+ was first detected using the Atacama Pathfinder Experiment 12m telescope toward the massive star-forming region Sagittarius B2(M) (*6*). H_2O^+ was found using the Herschel satellite toward the star-forming regions DR21, Sagittarius B2(M), and NGC 6334 (*7*). The protonated water molecule H_3O^+ was first detected much earlier, using the National Radio Astronomy Observatory 12m telescope toward Orion KL and OMC-1 (*8*, *9*). Furthermore, all of these molecular ions were found along the line of sight toward the submillimeter continuum source G10.6-0.4 (W31C) using the Herschel Heterodyne Instrument for the Far Infrared (*10*). Since OH^+ and H_2O^+ are known to react exothermically with H_2, both ions are believed to reside in environments with a low fraction of molecular to atomic hydrogen. The observed velocity profiles support this assumption (*11*). Apart from their crucial role in the gas-phase water chain, both OH^+ and H_2O^+ play key roles in the formation of oxygen-bearing molecules such as OH, CO, and other polyatomic molecules in the ISM (*4*).

To analyze the gas-phase water chain, most astronomical models use the rates that are reported in the University of Manchester Institute of Science and Technology (UMIST) database (*12*), which lists $k_1 = 1.01(\pm0.20) \times 10^{-9}$ cm^3 s^{-1} for reaction (1) and $k_2 = 6.4(\pm3.2) \times 10^{-10}$ cm^3 s^{-1} for reaction (2). These values are based on the experiments of Jones *et al.* (*13*) and Rakshit and Warneck (*14*), although the original work is almost never cited in the astronomical literature. The rate coefficients were measured in flow tube and drift chamber studies at 300 K, and typically, they are assumed to be independent of temperature. However, the measured values differ significantly from the energy-independent classical Langevin rate coefficient approximation (*15*), which yields values around $k_{1,2} \sim 1.5 \times 10^{-9}$ cm^3 s^{-1} for both reactions. Besides the experiments mentioned above, a number of additional room temperature values can be found in the literature, most of them being obtained in flow tube or drift chamber measurements. The published values show a significant scatter, and we refrain from addressing all of the individual measurements here (we will discuss the overall trends in Results and Discussion). In summary, the rate coefficients published for reaction (1) range from $k_1 = 8.6 \times 10^{-10}$ cm^3 s^{-1} (*16*) to $k_1 = 1.5 \times 10^{-9}$ cm^3 s^{-1} (*17*), while rate coefficients for reaction (2) range from $k_2 = 4.0 \times 10^{-10}$ cm^3 s^{-1} (*18*) to $k_2 = 1.4 \times 10^{-9}$ cm^3 s^{-1} (*17*), with additional values between these two extremes (*14*, *19*, *20*).

There is renewed interest in both reactions in recent years. Modern temperature-variable selected-ion flow-tube (SIFT) measurements were carried out between 200 to 600 K for reaction (1) (*21*) and from 100 to 600 K for reaction (2) (*22*). Both measurements show only a small variation of the rate coefficients with temperature, and in essence, the measured values agree with the rate coefficients listed in the UMIST database.

[1]Max-Planck-Institut für Kernphysik, 69117 Heidelberg, Germany. [2]Computation-based Science and Technology Research Center, Cyprus Institute, 20 Kavafi Street, Nicosia 2121, Cyprus. [3]Department of Chemical Engineering, Massachusetts Institute of Technology, 77 Massachusetts Avenue, Cambridge, MA 02139, USA. [4]Department of Chemistry and Chemical Biology, University of New Mexico, Albuquerque, NM 87131, USA. *Present address: Department of Physics, Indian Institute of Science Education and Research Tirupati, Andhra Pradesh 517507, India.
†Corresponding author. Email: sunil.phys@gmail.com (S.S.K.); ysuleyma@mit.edu (Y.V.S.); holger.kreckel@mpi-hd.mpg.de (H.K.)

Ng and co-workers (*23*–*25*) recently used a quite different experimental approach to shed light on reaction (2). They produced the H_2O^+ ion in specific rovibrational states using a state-of-the-art laser-pulsed field ionization method in the vacuum ultraviolet. These measurements mark a clear step forward as they provide state-selective absolute cross sections. However, since the translational energies are above 300 K, the implications for astronomical applications are not straightforward. Nevertheless, note that the absolute cross sections obtained for reaction (2), at energies near room temperature, are much higher than the commonly accepted values. The series of recent experiments have also sparked theoretical work (*26*–*28*), resulting in quasi-classical trajectory (QCT) and quantum dynamics (QD) calculations for both reactions.

It is generally acknowledged, however, that despite the fact that gas-phase water formation is a much-studied reaction chain, none of the previous techniques has reached sufficiently low temperatures to be truly applicable for interstellar conditions. Here, we present the first dedicated rate coefficient measurements for reactions (1) and (2) at temperatures below 100 K, performed in a temperature-variable radio-frequency ion trap. Ring-polymer molecular dynamics (RPMD) calculations accompany these measurements, taking into account quantum mechanical effects of nuclear motions that were absent in previous theoretical rate calculations.

RESULTS AND DISCUSSION

Laboratory measurements in a cryogenic ion trap

For our low-temperature measurements, we used a cryogenic 22-pole ion trap (*29*). Details on the experimental procedure and a schematic of the setup can be found in Methods. Briefly, OH^+, H_2O^+, and H_3O^+ ions are created inside a radiofrequency ion source (*30*) by electron impact on water vapor. The inset in Fig. 1 shows a typical mass spectrum. Owing to fast reactions of OH^+ and H_2O^+ with H_2O already inside the source, the H_3O^+ peak was usually dominant. Two consecutive quadrupole ion guides lead the ions into the 22-pole ion trap, facilitating efficient differential pumping and thus preventing H_2O or unwanted trace gases from traveling from the source region to the ion trap. Inside the 22-pole trap, we stored the ions in a large field-free central region to minimize radiofrequency heating. During storage, we continuously bled in unreactive helium buffer gas for cooling through precooled lines, reaching a typical number density of 10^{13} cm^{-3}. Since the 22-pole trap does not discriminate between different masses (for the mass range of interest in the present work), we simultaneously stored all ions coming from the source. To initiate the reactions of OH^+ and H_2O^+ with H_2, we let in small amounts of hydrogen gas through a precision valve. After a predefined time interval, we extracted the stored ions and analyzed them using a mass spectrometer. We took special care to calibrate the neutral H_2 density inside the trap, which is essential for determining absolute rate coefficients. For a given trap temperature and H_2 density, we monitored the decay of OH^+ and H_2O^+ as a function of storage time (Fig. 1, left) over many trap fillings. We fitted the resulting decay curves averaged over the trap fillings by a set of coupled differential equations (see the Supplementary Materials) to obtain the loss rates for each ion. Varying the H_2 density at a given temperature reveals a linear dependence, shown for two examples in the righthand panel of Fig. 1. For our low-temperature measurements presented here, we did not observe any contaminations in the mass spectra, and the dependence of the ion loss rates as a function of the hydrogen number density remained linear, with virtually no need for an axis offset (which would suggest an alternative loss mechanism). At higher temperatures (≥200 K), where the trap conditions become less "clean," we started to observe deviations, most likely from H_2O residual gas that is cryopumped less effectively at higher temperature. The linear fits to the loss rates yield the experimental rate coefficients for a fixed temperature. Table 1 lists the resulting values with relative 1σ statistical uncertainties. The determination of the H_2 number density

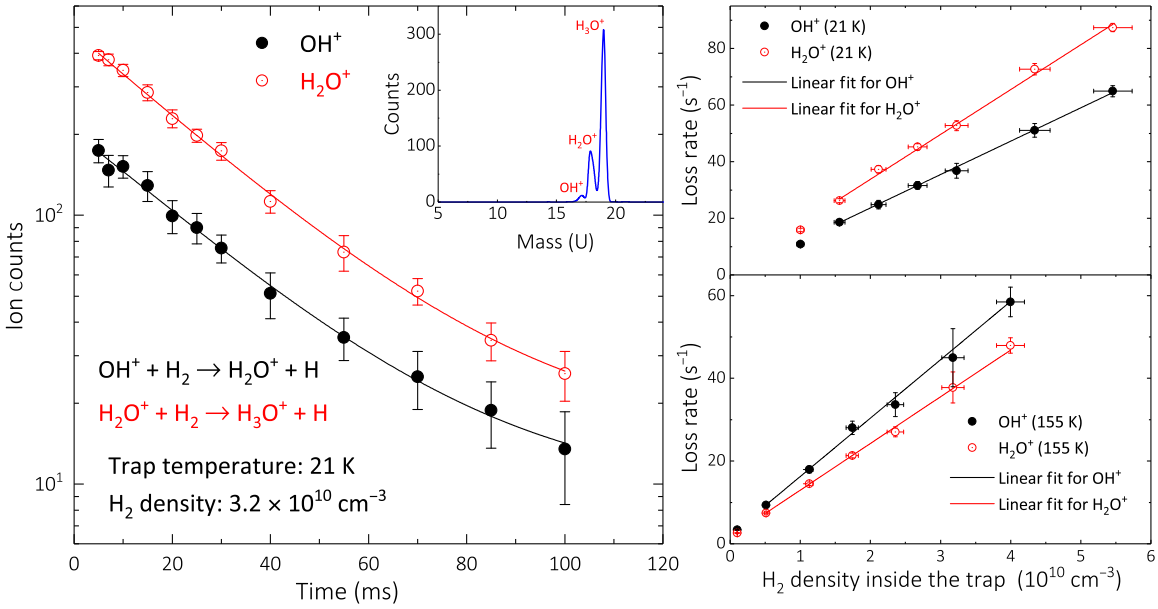

Fig. 1. Exemplary ion counts of OH^+ and H_2O^+ as a function of storage time and loss rates versus H_2 density. (**Left**) Decay curves of OH^+ and H_2O^+ as observed in the 22-pole trap at 21 K with a H_2 number density of 3.2×10^{10} cm^{-3}. The inset shows a spectrum of a typical initial mass distribution produced by the ion source. (**Right**) Loss rates for OH^+ and H_2O^+ as a function of H_2 density at two different temperatures. The data points at the lowest densities resulted from the residual H_2 in the trap, which varied with trap conditions and temperature. Those points, while fully consistent with the trend, were not included in the fit.

inside the ion trap dominates the uncertainty for the absolute scale of 20% (see the Supplementary Materials).

Theoretical calculation of the rate coefficients using RPMD

Theoretical calculations of the rate coefficients complement the experiment using a novel RPMD method (*31*). The accurate calculation of rate coefficients of reactions at low temperatures is still extremely difficult because of quantum effects such as tunneling, zero-point energy (ZPE), and resonances (*32*, *33*). Here, we computed the rate coefficients using the RPMDrate code (*34*), which takes advantage of the isomorphism between a statistical property of a quantum system and that of a fictitious classical ring polymer made of harmonically connected beads. Although RPMD calculations are performed by running classical trajectories, it offers an accurate account of quantum effects, which are particularly important for low-temperature reactions. Careful comparison between the RPMD approximation and exact quantum dynamical theory has been carried out recently for many prototypical reactions (*35*), including several barrierless complex-forming reactions similar to reactions (1) to (3), and the agreement has been very encouraging. Here, we focus on reactions (1) and (2), using recently developed full-dimensional potential energy surfaces based on fitting a large number of high-level ab initio data and augmented with analytical long-range interaction terms (*26*, *36*). Note that we did not distinguish the ortho- and para-H_2 in our calculations, and we assumed the H_2 rotational distribution to be Boltzmann. The details of the RPMD calculation can be found in the Supplementary Materials.

Table 1. Experimental and theoretical rate coefficients for reactions (1) and (2). Rate coefficients are given in units of 10^{-9} cm^3 s^{-1}. For the experimental values, the relative uncertainties are given in parentheses. Additional absolute uncertainties of 20% apply for all experimental data points. The experimental uncertainties correspond to 1 SD. Theoretical rate coefficients are converged to within a statistical error of ~10% (within 2 SDs).

	Experiment	
Trap temperature	k_1 $OH^+ + H_2 \rightarrow H_2O^+ + H$	k_2 $H_2O^+ + H_2 \rightarrow H_3O^+ + H$
21 K	1.22 (0.05)	1.57 (0.05)
55 K	1.33 (0.07)	1.53 (0.11)
72 K	1.41 (0.05)	1.52 (0.05)
103 K	1.35 (0.05)	1.39 (0.05)
155 K	1.32 (0.10)	1.17 (0.08)
	Theory (RPMD)	
50 K	1.54	1.56
100 K	—	1.51
300 K	1.48	—

Comparison of experiment/theory and with previous work

Table 1 and Fig. 2 show the results of the present experiment and calculations, together with previous measurements and calculations. Our low-temperature measurements, as well as theoretical calculations, indicate high rate coefficients for both reactions, almost approaching the classical Langevin collision limit. The present measurements of reaction (1) show higher values than the recent results of Martinez *et al.* (*21*), which only extend down to 200 K. Within the combined error bars, however, they can be regarded consistent. The RPMD results at 50 K are in excellent agreement with the current experimental values, and at 300 K RPMD, the error bar overlaps with the previous

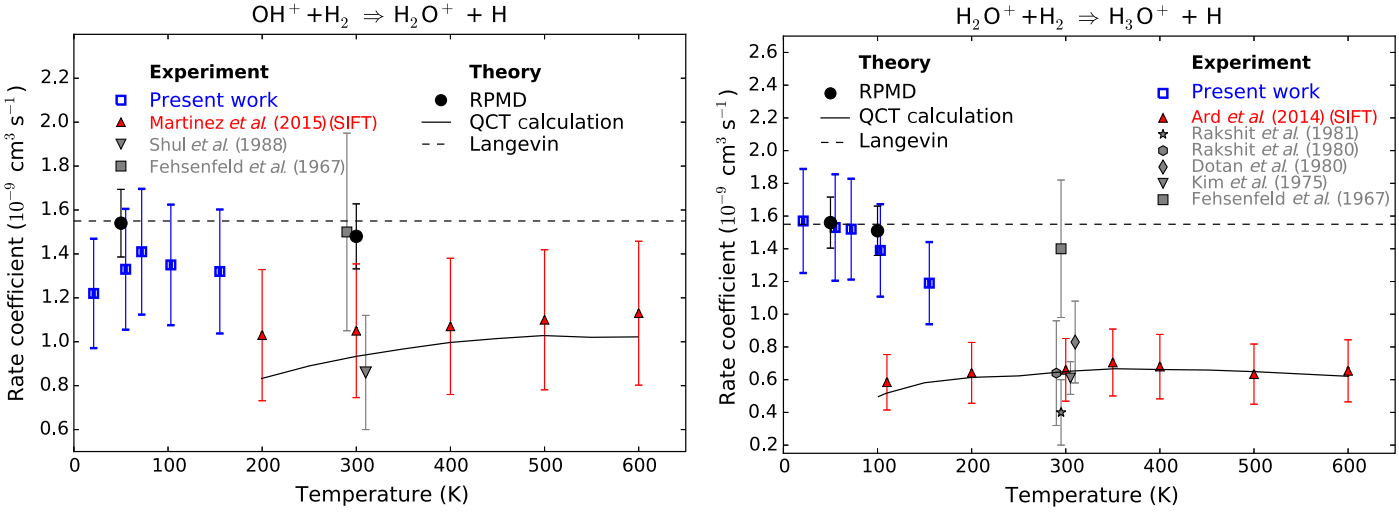

Fig. 2. Comparison of the present measured and calculated rate coefficients for the reactions of OH^+ and H_2O^+ with H_2 and previous measurements, QCT calculations, and the Langevin rate coefficient. For the present experimental work and the SIFT results of (*21*) and (*22*), we added the respective relative and absolute uncertainties in quadrature to depict absolute uncertainties for a fair comparison. The uncertainties for the present RPMD calculations represent the convergence limit within two SDs. Also shown are previous room temperature measurements; for clarity, they are shifted in steps of 10 K. Theoretical calculations (RPMD and QCT) were performed using potential energy surfaces (PESs) from (*26*, *36*). References for previous room temperature data are as follows: Shul *et al.* (1988) (*16*), Fehsenfeld *et al.* (1967) (*17*), Rakshit *et al.* (1981) (*18*), Rakshit *et al.* (1980) (*14*), Dotan *et al.* (1980) (*20*), and Kim *et al.* (1975) (*19*). Note that the measurements of Dotan *et al.* are actually energy-resolved, extend to kinetic center-of-mass collision energies of up to 0.3 eV (corresponding to k_BT = 3500 K), and show a slow monotonic decrease. Since the present work is concerned primarily with the low-temperature regime, we only show their lowest energy data point for clarity.

experimental results. As shown in the Supplementary Materials (fig. S2), the free-energy barrier for reaction (1) is very small (below 0.1 kcal/mol) at this temperature, suggesting a loose bottleneck. At the same time, the ring polymer transmission coefficients (or real-time recrossing factor) require picoseconds of propagation to reach plateau values, which are significantly below unity when reaching the product region (see the Supplementary Materials), underscoring its importance in the total RPMD rate coefficient calculation. The QCT calculations presented in (*21*) are distinctly lower at both low and room temperatures. QCT's reliability is sometimes uncertain (*35*, *37*), particularly at low energies and temperatures, as this approximation completely ignores important quantum effects such as tunneling, resonances, and—presumably more importantly for the present essentially barrierless reactions (1) and (2)—ZPE conservation along the reaction path (see the energy diagrams in the Supplementary Materials). For instance, for another complex-formation astrochemical reaction in the H_5^+ system, it was recently shown that the ZPE leakage in QCT simulations can lead to strong deviations from experimental data at low temperatures (*37*). By contrast, RPMD was shown to be immune to these shortcomings as it accurately treats the ZPE along the reaction coordinate. As discussed in the Supplementary Materials, the higher temperature gives rise to a slightly higher free-energy barrier (0.6 kcal/mol) in the entrance channel, but it is offset by a smaller recrossing factor. The temperature dependence of k_1 is negligible, again in agreement with the experiment.

For reaction (2), the experiment-theory agreement near 50 and 100 K is also excellent. As shown in the Supplementary Materials, the free-energy barrier for this reaction is again almost null, supporting the capture model. However, we see a distinct discrepancy between our results and the previous SIFT measurements (*22*), which are lower in the overlapping temperature regime. Most of the previous room temperature experiments (also shown in Fig. 2) resulted in lower rate coefficients; however, the temperature trend observed in the current results may be consistent with these findings. One potentially significant difference between our data and almost all previous studies [except for the room temperature ion cyclotron resonance measurements of Kim *et al.* (*19*)] is the pressure regime. While the number densities in all experiments are orders of magnitude higher than in interstellar space, the H_2 density in our studies was below 10^{11} cm^{-3}, and the helium buffer gas density was on the order of 10^{13} cm^{-3}. These conditions are safely within the two-body regime. Most studies in flow tubes and drift chambers are carried out at helium pressures around 1 torr, resulting in densities on the order of 10^{16} cm^{-3}, at least three orders of magnitude higher than in the present work. For some critical reactions (that have a long-lived collision complex), high number densities can influence the rate coefficients significantly; for example, the electron recombination of H_3^+ in flow tubes seems to be dominated by ternary effects (*38*, *39*). However, in the present case, one would probably expect that collisions with helium would stabilize the collision complex and increase the rate coefficient rather than decrease it. Therefore, we presently have no compelling explanation for the discrepancy between the present work and the recent SIFT experiments (*22*) at temperatures below room temperature.

As we have not used a dedicated catalytic converter to modify the H_2 ortho/para ratio in the experiment, we expect ortho-H_2 to be somewhat overpopulated for the low-temperature experimental points in both reactions, when compared to the Boltzmann distribution that we assumed in the calculations. However, a previous QD study of reaction (1) showed that the ortho and para forms of H_2 have similar reactivity (*28*). Furthermore, since we observe for both reactions rate coefficients that are very close to the classical capture rate and vary only weakly with temperature, we do not anticipate a strong influence of the nuclear spin.

CONCLUSION

Countless astronomical models and observational analyses have used the rate coefficients for reactions (1) and (2). Assessing the impact of the much higher rate coefficient for reaction (2) (compared to the previously accepted room temperature value) for different astronomical environments is beyond the scope of this work. On a broader scope, the combined experimental and theoretical study of the prototypical ion-molecule reactions considered here has implications even beyond the interstellar gas-phase water and oxygen networks. While modern interstellar chemistry codes often contain hundreds of rate coefficients (most of them for ion-neutral processes), only a handful of these reactions have been measured at the relevant temperatures. Consequently, interstellar gas-phase models continue to rely on extrapolated or guessed values for most of the reactions, rendering them vulnerable to the propagation of large errors and uncertainties. Here, we present laboratory measurements and accurate calculations for two key astrophysical ion-neutral reactions using methods for both experiment and theory that are suitable for the extreme temperatures and densities of interstellar environments. Accurate measurements of absolute rate coefficients under true interstellar conditions still pose a great challenge. In view of the growing molecular complexity that is uncovered by modern instruments such as the Atacama Large Millimeter/submillimeter Array, it is therefore crucial to benchmark promising theoretical methods, as it is apparent that the laboratory efforts alone will be outpaced by the observational demands.

In summary, our low-temperature measurements find that both OH^+ and H_2O^+ ions react very fast with molecular hydrogen, with rate coefficients very close to the Langevin limit. The rate coefficients for both reactions are well reproduced by our RPMD calculations. These findings corroborate the assumption that both molecular ions have to reside in interstellar environments with low H_2 density. The perfect agreement of the low-temperature experimental and theoretical data is very promising. Contrasted by the discrepancy with previous QCT calculations, it indicates that it is essential to include quantum effects when considering reactions at interstellar temperature, even for seemingly nondiscriminative exothermic ion-neutral processes.

METHODS

Measurement procedure

The initial OH^+ and H_2O^+ ions were produced in the storage ion source by electron impact on water vapor (for this purpose, a small reservoir of distilled water was connected to one of the gas inlets of the source). We typically accumulated and stored the ions for a few milliseconds inside the source before extraction to thermalize their translational motion after ionization, which increases the capture efficiency in the 22-pole trap. The mass spectrum of the ions generated in the source, and transported through the 22-pole trap without storing, is shown in the inset of Fig. 1. OH^+, H_2O^+, and H_3O^+ were readily produced inside the source, the latter being formed after ionized water H_2O^+ or OH^+ reacted with neutral H_2O inside the source. Therefore, the H_3O^+ signal was typically the strongest peak coming from the source, and OH^+ was the weakest. The mass spectrum remained unchanged when

we stored the ions for a short period of time inside the ion trap without letting in any gas. All of the ions coming from the source were stored simultaneously inside the 22-pole trap, as there is basically no mass separation in the trap for these comparatively light masses.

During the experiments, we continuously bled in nonreactive helium buffer gas for cooling (typical density, 10^{13} cm^{-3}) and H_2 reactant gas (typical densities, 10^{10} to 10^{11} cm^{-3}) while, at the same time, monitoring the decay of the OH^+ and H_2O^+ ions as a function of storage time (Fig. 1, left). For initial measurements, we kept the total number of stored ions low (approximately ~500) to confirm that all OH^+ and H_2O^+ ions ended up as H_3O^+ in reactions with H_2. For a larger number of ions, the H_3O^+ signal—being the strongest peak right from the start—will saturate, as the ions were extracted from the trap in a bunch that is only several 10 μs long. For more than a thousand ions per bunch, their signal piled up in the detector, and single-particle counting was no longer accurate. However, since the initial OH^+ counts were too small to collect enough statistics in this mode, we increased the number of stored ions to a few thousand, at the expense of saturating the H_3O^+ signal, which was not essential for determining the rate coefficients. We performed various cross-checks between measurements at small and large number of ions and observed no difference in the decay curves or resulting rate coefficients. The intrinsic lifetimes of the stored ions inside the trap were on the order of several seconds and thus much longer than the decay times that we aimed to determine.

For our measurements, we varied the trap temperature between ~20 and ~150 K and the H_2 number density between 1×10^9 and 1×10^{11} cm^{-3}. For each temperature and density, we recorded the decay curves of OH^+ and H_2O^+, averaging usually over at least 20 trap fillings per storage time bin.

RPMD rate theory

The RPMD rate theory is a relatively new approach to approximate quantum mechanical effects of nuclear motions in chemical dynamics studies, developed (*31*) and extensively benchmarked over the past decade (*35*). This method is based on the isomorphism between a quantum system and its n classical copies forming a necklace and coupled to the nearest neighbors via harmonic interactions. The classical isomorphism allows switching from purely quantum formalism to purely classical formalism and is formally an exact approach to calculate various static properties in which n (number of beads in the necklace) is a convergence parameter. The real-time dynamics of this necklace ("ring polymer") represents an ad hoc idea of RPMD (*31*) to calculate approximately real-time correlation functions responsible for describing various dynamical processes, including chemical reactions (*35*). Through extensive study of various small gas-phase chemical reactions, it has been shown (*35*) that such an approximation to real-time dynamics allows accurate treatment of quantum mechanical effects of nuclear motions and provides very reliable and accurate estimates of thermal rate constants for different energy profiles along chemical reaction paths and temperatures. The key features of RPMD that lead to this success are (i) exact classical high-temperature limit, (ii) independence of the choice of transition state dividing surface, and (iii) connection to various transition state theories in the short-time limit (*35*). Here, we used the PESs for the title reactions (1) and (2) from (*26*, *36*).

SUPPLEMENTARY MATERIALS

Supplementary material for this article is available at http://advances.sciencemag.org/cgi/content/full/4/6/eaar3417/DC1

Supplementary Materials and Methods

fig. S1. Schematic of the experimental setup.

fig. S2. Potential of mean force [$W(\xi)$] and ring polymer recrossing factor [$\kappa(t)$] for the $OH^+ + H_2$ reaction at 50 and 300 K.

fig. S3. Potential of mean force [$W(\xi)$] and ring polymer recrossing factor [$\kappa(t)$] for the $H_2O^+ + H_2$ reaction at 50 and 100 K.

fig. S4. Histograms of final distances between the centers of mass of the products.

fig. S5. Schematic illustration of the reaction paths.

table S1. Rate coefficients (in 10^{-9} cm^3 s^{-1}) for the $OH^+ + H_2$ and $H_2O^+ + H_2$ reactions calculated using centroid-density quantum transition state theory (k_{QTST}) and RPMD (k_{RPMD}).

table S2. Input parameters for the RPMDrate calculations on the $OH^+ + H_2$ and $H_2O^+ + H_2$ reactions.

References (*40*, *41*)

REFERENCES AND NOTES

1. A. C. Cheung, D. M. Rank, C. H. Townes, D. D. Thornton, W. J. Welch, Detection of water in interstellar regions by its microwave radiation. *Nature* **221**, 626–628 (1969).
2. F. C. Gillett, W. J. Forrest, Spectra of the Becklin-Neugebauer point source and the Kleinmann-Low nebula from 2.8 to 13.5 microns. *Astrophys. J.* **179**, 483–491 (1973).
3. E. L. Gibb, D. C. B. Whittet, A. C. A. Boogert, A. G. G. M. Tielens, Interstellar Ice: The infrared space observatory legacy. *Astrophys. J. Suppl.* **151**, 35 (2004).
4. D. Hollenbach, M. J. Kaufman, D. Neufeld, M. Wolfire, J. R. Goicoechea, The chemistry of interstellar OH^+, H_2O^+, and H_3O^+: Inferrring the cosmic-ray ionization rates from observations of molecular ions. *Astrophys. J.* **754**, 105 (2012).
5. N. Indriolo, D. A. Neufeld, M. Gerin, P. Schilke, A. O. Benz, B. Winkel, K. M. Menten, E. T. Chambers, J. H. Black, S. Bruderer, E. Falgarone, B. Godard, J. R. Goicoechea, H. Gupta, D. C. Lis, V. Ossenkopf, C. M. Persson, P. Sonnentrucker, F. F. S. van der Tak, E. F. van Dishoeck, M. G. Wolfire, F. Wyrowski, Herschel survey of galactic OH^+, H_2O^+, and H_3O^+: Probing the molecular hydrogen fraction and cosmic-ray ionization rate. *Astrophys. J.* **800**, 40 (2015).
6. F. Wyrowski, K. M. Menten, R. Güsten, A. Belloche, First interstellar detection of OH^+. *Astron. Astrophys.* **518**, A26 (2010).
7. V. Ossenkopf, H. S. P. Müller, D. C. Lis, P. Schilke, T. A. Bell, S. Bruderer, E. Bergin, C. Ceccarelli, C. Comito, J. Stutzki, A. Bacman, A. Baudry, A. O. Benz, M. Benedettini, O. Berne, G. Blake, A. Boogert, S. Bottinelli, F. Boulanger, S. Cabrit, P. Caselli, E. Caux, J. Cernicharo, C. Codella, A. Coutens, N. Crimier, N. R. Crockett, F. Daniel, K. Demyk, P. Dieleman, C. Dominik, M. L. Dubernet, M. Emprechtinger, P. Encrenaz, E. Falgarone, K. France, A. Fuente, M. Gerin, T. F. Giesen, A. M. di Giorgio, J. R. Goicoechea, P. F. Goldsmith, R. Güsten, A. Harris, F. Helmich, E. Herbst, P. Hily-Blant, K. Jacobs, T. Jacq, C. Joblin, D. Johnstone, C. Kahane, M. Kama, T. Klein, A. Klotz, C. Kramer, W. Langer, B. Lefloch, C. Leinz, A. Lorenzani, S. D. Lord, S. Maret, P. G. Martin, J. Martin-Pintado, C. McCoey, M. Melchior, G. J. Melnick, K. M. Menten, B. Mookerjea, P. Morris, J. A. Murphy, D. A. Neufeld, B. Nisini, S. Pacheco, L. Pagani, B. Parise, J. C. Pearson, M. Pérault, T. G. Phillips, R. Plume, S.-L. Quin, R. Rizzo, M. Röllig, M. Salez, P. Saraceno, S. Schlemmer, R. Simon, K. Schuster, F. F. S. van der Tak, A. G. G. M. Tielens, D. Teyssier, N. Trappe, C. Vastel, S. Viti, V. Wakelam, A. Walters, S. Wang, N. Whyborn, M. van der Wiel, H. W. Yorke, S. Yu, J. Zmuidzinas, Detection of interstellar oxidaniumyl: Abundant H_2O^+ towards the star-forming regions DR21, Sgr B2, and NGC6334. *Astron. Astrophys.* **518**, L111 (2010).
8. J. M. Hollis, E. B. Churchwell, E. Herbst, F. C. De Lucia, An interstellar line coincident with the P(2,I)transition of hydronium (H_3O^+). *Nature* **322**, 524–526 (1986).
9. A. Wootten, F. Boulanger, M. Bogey, F. Combes, P. J. Encrenaz, M. Gerin, L. Ziurys, A search for interstellar H_3O^+. *Astron. Astrophys.* **166**, L15–L18 (1986).
10. M. Gerin, M. De Luca, J. Black, J. R. Goicoechea, E. Herbst, D. A. Neufeld, E. Falgarone, B. Godard, J. C. Pearson, D. C. Lis, T. G. Phillips, T. A. Bell, P. Sonnentrucker, F. Boulanger, J. Cernicharo, A. Coutens, E. Dartois, P. Encrenaz, T. Giesen, P. F. Goldsmith, H. Gupta, C. Gry, P. Hennebelle, P. Hily-Blant, C. Joblin, M. Kazmierczak, R. Kolos, J. Krelowski, J. Martin-Pintado, R. Monje, B. Mookerjea, M. Perault, C. Persson, R. Plume, P. B. Rimmer, M. Salez, M. Schmidt, J. Stutzki, D. Teyssier, C. Vastel, S. Yu, A. Contursi, K. Menten, T. Geballe, S. Schlemmer, R. Shipman, A. G. G. M. Tielens, S. Philipp-May, A. Cros, J. Zmuidzinas, L. A. Samoska, K. Klein, A. Lorenzani, Interstellar OH^+, H_2O^+ and H_3O^+ along the sight-line to G10.6–0.4. *Astron. Astrophys.* **518**, L110 (2010).
11. D. A. Neufeld, J. R. Goicoechea, P. Sonnentrucker, J. H. Black, J. Pearson, S. Yu, T. G. Phillips, D. C. Lis, M. De Luca, E. Herbst, P. Rimmer, M. Gerin, T. A. Bell, F. Boulanger, J. Cernicharo, A. Coutens, E. Dartois, M. Kazmierczak, P. Encrenaz, E. Falgarone, T. R. Geballe, T. Giesen, B. Godard, P. F. Goldsmith, C. Gry, H. Gupta, P. Hennebelle, P. Hily-Blant, C. Joblin, R. Kołos, J. Krełowski, J. Martín-Pintado, K. M. Menten, R. Monje, B. Mookerjea, M. Perault, C. Persson, R. Plume, M. Salez, S. Schlemmer, M. Schmidt, J. Stutzki, D. Teyssier, C. Vastel, A. Cros, K. Klein, A. Lorenzani, S. Philipp, L. A. Samoska, R. Shipman, A. G. G. M. Tielens, R. Szczerba, J. Zmuidzinas, *Herschel*/HIFI observations of interstellar OH^+ and H_2O^+ towards W49N: A probe of diffuse clouds with a small molecular fraction. *Astron. Astrophys.* **521**, L10 (2010).

12. D. McElroy, C. Walsh, A. J. Markwick, M. A. Cordiner, K. Smith, T. J. Millar, The UMIST database for astrochemistry 2012. *Astron. Astrophys.* **550**, A36 (2013).
13. J. D. C. Jones, K. Birkinshaw, N. D. Twiddy, Rate coefficients and product ion distributions for the reactions of OH^+ and H_2O^+ with N_2, O_2, NO, N_2O, Xe, CO, CO_2, H_2S and H_2 at 300 K. *Chem. Phys. Lett.* **77**, 484–488 (1981).
14. A. B. Rakshit, P. Warneck, Reactions of CO_2^+, $CO_2CO_2^+$ and H_2O^+ ions with various neutral molecules. *J. Chem. Soc. Faraday Trans. 2* **76**, 1084–1092 (1980).
15. G. Gioumousis, D. P. Stevenson, Reactions of gaseous molecule Ions with gaseous molecules. V. Theory. *J. Chem. Phys.* **29**, 294–299 (1958).
16. R. J. Shul, R. Passarella, L. T. Difazio, R. G. Keesee, A. W. Castleman, Ion molecule reactions involving H_3O^+, H_2O^+, and OH^+ at thermal energy. *J. Phys. Chem.* **92**, 4947–4951 (1988).
17. F. C. Fehsenfeld, A. L. Schmeltekopf, E. E. Ferguson, Thermal-energy ion-neutral reaction rates 7. Some hydrogen-atom abstraction reactions. *J. Chem. Phys.* **46**, 2802–2808 (1967).
18. A. B. Rakshit, P. Warneck, A drift chamber study of the reaction $ArH^+ + H_2 \rightarrow H^{+3}$ + Ar and related reactions. *J. Chem. Phys.* **74**, 2853–2859 (1981).
19. J. K. Kim, L. P. Theard, W. T. Huntress, ICR studies of some hydrogen-atom abstraction reaction: $X^+ + H_2 \rightarrow XH^+ + H$. *J. Chem. Phys.* **62**, 45–52 (1975).
20. I. Dotan, W. Lindinger, B. Rowe, D. W. Fahey, F. C. Fehsenfeld, D. L. Albritton, Rate constants for the reactions of H_2O^+ with NO_2, O_2, NO, C_2H_4, CO, CH_4, and H_2 measured at relative kinetic energies 0.04–2 eV. *Chem. Phys. Lett.* **72**, 67–70 (1980).
21. O. Martinez, S. G. Ard, A. Li, N. S. Shuman, H. Guo, A. A. Viggiano, Temperature-dependent kinetic measurements and quasi-classical trajectory studies for the $OH^+ + H_2/D_2 \rightarrow H_2O+/HDO^+ + H/D$ reactions. *J. Chem. Phys.* **143**, 114310 (2015).
22. S. G. Ard, A. Li, O. Martinez Jr., N. S. Shuman, A. A. Viggiano, H. Guo, Experimental and theoretical kinetics for the $H_2O^+ + H_2/D_2 \rightarrow H_3O^+/H_2DO^+ + H/D$ reactions: Observation of the rotational Effect in the temperature dependence. *J. Phys. Chem. A* **118**, 11485–11489 (2014).
23. Y. Xu, B. Xiong, Y. C. Chang, C. Y. Ng, Communication: Rovibrationally selected absolute total cross sections for the reaction $H_2O^+(X^2B_1; v_1^+v_2^+v_3^+=000; N^+_{Ka+Kc+}) + D_2$: Observation of the rotational enhancement effect. *J. Chem. Phys.* **137**, 241101 (2012).
24. Y. Xu, B. Xiong, Y. C. Chang, C. Y. Ng, The translational, rotational, and vibrational energy effects on the chemical reactivity of water cation $H_2O^+(X^2B_1)$ in the collision with deuterium molecule D_2. *J. Chem. Phys.* **139**, 024203 (2013).
25. A. Li, Y. Li, H. Guo, K.-C. Lau, Y. Xu, Bo Xiong, Y.-C. Chang, C. Y. Ng, Communication: The origin of rotational enhancement effect for the reaction of $H_2O^+ + H_2$ (D_2). *J. Chem. Phys.* **140**, 011102 (2014).
26. A. Li, H. Guo, A nine-dimensional ab initio global potential energy surface for the $H_2O^+ + H_2 \rightarrow H_3O^+ + H$ reaction. *J. Chem. Phys.* **140**, 224313 (2014).
27. H. Song, A. Li, H. Guo, Y. Xu, B. Xiong, Y.-C. Chang, C. Y. Ng, Comparison of experimental and theoretical quantum-state-selected integral cross sections for the $H_2O^+ + H_2$ (D_2) reactions in the collision energy range of 0.04-10.00 eV. *Phys. Chem. Chem. Phys.* **18**, 22509–22515 (2016).
28. H. Song, A. Li, H. Guo, Rotational and isotopic effects in the $H_2 + OH^+ \rightarrow H + H_2O^+$ reaction. *J. Phys. Chem. A* **120**, 4742–4748 (2016).
29. D. Gerlich, Inhomogeneous RF-fields - A versatile tool for the study of processes with slow ions. *Adv. Chem. Phys.* **82**, 1–176 (1992).
30. D. Gerlich, thesis, University Freiburg (1971).
31. S. Habershon, D. E. Manolopoulos, T. E. Markland, T. F. Miller III, Ring-polymer molecular dynamics: Quantum effects in chemical dynamics from classical trajectories in a extended phase space. *Annu. Rev. Phys. Chem.* **64**, 387–413 (2013).
32. J. Daranlot, M. Jorfi, C. Xie, A. Bergeat, M. Costes, P. Caubet, D. Xie, H. Guo, P. Honvault, K. M. Hickson, Revealing atom-radical reactivity at low temperature through the N + OH reaction. *Science* **334**, 1538–1541 (2011).
33. M. Tizniti, S. D. Le Picard, F. Lique, C. Berteloite, A. Canosa, M. H. Alexander, I. R. Sims, The rate of the F + H_2 reaction at very low temperatures. *Nat. Chem.* **6**, 141–145 (2014).
34. Y. V. Suleimanov, J. W. Allen, W. H. Green, RPMDrate: Bimolecular chemical reaction rates from ring polymer molecular dynamics. *Comput. Phys. Commun.* **184**, 833–840 (2013).
35. Y. V. Suleimanov, F. J. Aoiz, H. Guo, Chemical reaction rate coefficients from ring polymer molecular dynamics: Theory and practical applications. *J. Phys. Chem. A* **120**, 8488–8502 (2016).
36. A. Li, H. Guo, A full-dimensional ab initio global potential energy surface of $H_3O^+(\tilde{a}^3A)$ for the $OH^+(\tilde{X}^3\Sigma^-) + H_2(\tilde{X}^1\Sigma_g^+) \rightarrow H(^2S) + H_2O^+(\tilde{X}^2B_1)$ reaction. *J. Phys. Chem. A* **118**, 11168–11176 (2014).
37. Y. V. Suleimanov, A. Aguado, S. Gómez-Carrasco, O. Roncero, A ring polymer molecular dynamics approach to study the transition between statistical and direct mechanisms in the $H_2 + H_3+ \rightarrow H_3+ + H_2$ reaction. *J. Phys. Chem. Lett.* **9**, 2133–2137 (2018).
38. H. Kreckel, D. Bing, S. Reinhardt, A. Petrignani, M. Berg, A. Wolf, Chemical probing spectroscopy of H_3^+ above the barrier to linearity. *J. Chem. Phys.* **129**, 164312 (2008).
39. R. Johnsen, P. Rubovič, P. Dohnal, M. Hejduk, R. Plašil, J. Glosík, Ternary recombination of H_3^+ and D_3^+ with electrons in He–H_2 (D_2) plasmas at temperatures from 50 to 300 K. *J. Phys. Chem. A* **117**, 9477–9485 (2013).
40. F. Pavese, G. Molinar Min Beciet, *Modern Gas-Based Temperature and Pressure Measurements* (Springer, ed. 2, 2013).
41. G. A. Miller, On the calculation of thermal transpiration. *J. Phys. Chem.* **67**, 1359–1361 (1963).

Acknowledgments: We thank A. A. Viggiano for the helpful comments and stimulating discussion. **Funding:** S.S.K. was supported by the Deutsche Forschungsgemeinschaft (DFG) within the DFG Priority Program 1573 "Physics of the Interstellar Medium" (contract no. KR 4617/1-1). F.G. and H.K. were supported by the European Research Council under grant agreement "Astrolab" no. StG 307163. Y.V.S. thanks the European Regional Development Fund and the Republic of Cyprus for the support through the Research Promotion Foundation (Project Cy-Tera NEA ΥΠΟΔΟΜΗ/ΣΤΡΑΤ/0308/31). Y.V.S. also acknowledges the support of the European Cooperation in Science and Technology Chemistry and Molecular Sciences and Technologies–Action CM1401 (Our Astro-Chemical History). H.G. acknowledges support from the U.S. Air Force Office of Scientific Research (FA-9550-15-1-0305). The support by the Max Planck Society is gratefully acknowledged. **Author contributions:** S.S.K. and H.K. designed and conceived the experimental research. S.S.K. and F.G. carried out the preparation of the setup and performed the measurements. H.G. and Y.V.S. devised the theoretical strategy and parameters and verified and interpreted the theoretical results. Y.V.S. wrote the RPMD code and carried out the rate coefficient calculations. **Competing interests:** The authors declare that they have no competing interests. **Data and materials availability:** All data needed to evaluate the conclusions in the paper are present in the paper and/or the Supplementary Materials. Additional data related to this paper may be requested from the authors.

Submitted 27 October 2017
Accepted 15 May 2018
Published 22 June 2018
10.1126/sciadv.aar3417

Citation: S. S. Kumar, F. Grussie, Y. V. Suleimanov, H. Guo, H. Kreckel, Low temperature rates for key steps of interstellar gas-phase water formation. *Sci. Adv.* **4**, eaar3417 (2018).

Low temperature rates for key steps of interstellar gas-phase water formation

Sunil S. Kumar, Florian Grussie, Yury V. Suleimanov, Hua Guo and Holger Kreckel

Sci Adv **4** (6), eaar3417.
DOI: 10.1126/sciadv.aar3417